Norwegian University
of Life Sciences

Master's Thesis 2019 30 ECTS
Faculty of Environmental Sciences and
Natural Resource Management (MINA)

Estimation of Production Losses due to Icing on Wind Turbines at Kvitfjell Wind Farm

Håkon Albrigtsen Kjersem
Renewable energy

Acknowledgments

As a part of the master program Renewable Energy at Norwegian University of Life Sciences, this master thesis marks the end of my five years education.

This thesis within wind power is written in collaboration with Kvitfjell wind farm which is, as of May 2019, a pre-operational wind farm. The assignment is given by Kvitfjell wind farm project group (associated with TÜV) and the results will hopefully contribute to a more accurate AEP estimation.

I would like to sincerely thank my supervisor associate professor Arne Reidar Gravdahl for guidance through this project and for letting me dispose resources at WindSim. A big thanks to Dr. Matthew Homola for bringing me up to speed on icing physics which I did not know anything about when I started this project. Thanks to Dipl.-Ing. Andreas Schmid at TÜV for providing the necessary data and enduring all my questions.

Windographer is greatly acknowledged for being so kind and suppling me with their software for the data processing. Kathryn Donnelly is kindly acknowledged for her help with proofreading. I also need to make a big thanks to Alexander Dybvad for being my sparring mate during this project. Finally, a big thanks to my classmate for giving me an awesome inspiring time at NMBU and my family for the support and encouragement through these last months.

Norwegian University of Life Sciences

Ås, May 10, 2019

Håkon Albrigtsen Kjersem

Abstract

Wind farms in cold climates are known for their challenge's with lowered performance due to icing on wind turbine blades, but there is little knowledge around the correlation between wind, ice and energy production which is of great importance for investors. To increase accuracy and knowledge of production losses from icing, a method for ice modelling based on measured data from met mast is established.

In this thesis the production losses due to icing on wind turbine blades at Kvitfjell wind farm is investigated in the period of July 2014 – January 2016 through use of CFD-simulation. Two ice scenarios are established, and the largest production losses is found to be 9,50 % of total energy production in the worst-case scenario. The more likely scenario is estimated to have a production loss at 4,75 %.

There are uncertainties around how well the ice model manages to capture the actual ice conditions as there may be large variation in atmospheric icing within the wind farm and it is assumed a flat reduction in power curve. Implementation of more data would increase the accuracy of the model as well as measurements of cloud frequency, ice shape- and type.

Sammendrag

Vindparker i kaldt klima er kjent for sin utfordring med redusert ytelse grunnet ising på vindturbinblad, men det er til tross lite kunnskap rundt sammenhengen mellom vind-, is- og energiproduksjon, som er av stor betydning for investorer. For å øke nøyaktigheten og kunnskapen om produksjonstap fra ising, er en metode for is modellering basert på målte data fra met mast etablert.

I denne oppgaven undersøkes produksjonstapene som følge av isdannelse på vindturbinblader ved Kvitfjell vindkraftverk i perioden juli 2014 - januar 2016 ved bruk av CFD-simulering. To is-scenarioer er etablert, og det største produksjonstapet er funnet til å være 9,50 % av den samlede energiproduksjonen i det verste utfalls-scenarioet. Det mer sannsynlige scenarioet er beregnet til å ha et produksjonstap på 4,75 %.

Det er usikkerhet rundt hvor godt is-modellen klarer å fange de faktiske isforholdene, da det kan være store variasjoner i atmosfærisk ising innad vindparken, og det antas en flat reduksjon i effektkurven. Implementering av mer data vil øke nøyaktigheten av modellen, så vel som målinger av skyforekomst, is-form og -type.

Contents

Abbreviations and Definitions

CC	Cold climates
AEP	Annual Energy Production
IEA	International Energy Agency
CFD	Computational Fluid Dynamics
LWC	Liquid Water Content
CCN	Cloud Condensation Nuclei
RH	Relative Humidity
OWI	Operation With Ice
Atmospheric icing	Periods where atmospheric condition enables ice growth.
Ice losses	Production losses induced by icing on rotor blade.
Accretion	Period of an ice event where ice is growing.
Persistence	Period of an ice event where ice remains without any ice growth.
Ablation	Period of an ice event where ice is removed through natural processes.
Shedding	Ice removal process where pieces of ice breaks off.

1. Introduction

1.1 Wind Power in Cold Climates

Wind energy has in the recent years been one of the fastest growing electricity production source in the world. Until now most of the wind farms have been built at temperate or offshore sites. However, due to decreasing areas with temperate location and offshore wind farm being more expensive than predicted, cold climates (CC) site are becoming more desirable because of low population density and good wind conditions (Bredesen et al., 2017).

At the end of 2015 there were approximately 127 GW installed capacity in CC. At the same time the growth rate of installed capacity in CC were 12 GW/year compared to offshore wind with 4 GW/year (Lehtomaki, 2016). With this tendency of growth forecast it is important to have the knowledge and tools for estimating accurate average annual energy production (AEP) in CC to fully utilize the wind resource. One of the main challenges of estimating AEP in CC is the uncertainty concerning production losses due to icing on wind turbine blades. AEP is usual based on wind speed calculation that neglect reduced performance from ice which leads to an overestimation.

1.2 Former Research on Problems Related to Icing on Wind Turbines

When it comes to wind turbines there are numerus aspects that are affected by icing and not only the performance. To better understand how wind turbines are influenced by icing we need to look at other fields with known ice related problems. The aircraft industry and power transmission industry are two quite different fields which both have challenges concerning icing and they both represent similar challenges with icing to those found on wind turbines. Wind turbine blades have the same attributes as found in aircraft wings when it comes to ice collection which is higher then found in stationary objects. However, wind turbines are bound to one specific placement when first erected, just as a power mast. Wind turbines must therefore endure the climate at the location and cannot navigate around unwanted icy weather to avoid it, as aircraft can (Homola, 2011).

As it is not possible to avoid the ice related problems which brings uncertainties to energy production, it is a hindrance for investments. Investors expect higher rate of return as they take the risk of investing in such projects. As a step to increase knowledge of ice related problem on wind turbines and reduce the risk, International Energy Agency (IEA) has published a

recommended practise study on wind energy projects in cold climates (Bredesen et al., 2017; Homola, 2011).

1.2.1 Estimation of Ice

The first step suggested by IEA is to identify what kind of CC the site is, low temperature climate or icing climate. For icing climates, such as found at Kvitfjell, an early indication of a sites icing severity is given by an ice classification table, seen in Table 1. By considering meteorological icing or instrumental icing which correspond to an ice class, a gross annual production loss can be obtained. The table refers to long term icing conditions and may not be representative for single winters.

Table 1: IEA Ice classification (Barber et al., 2011)

IEA Ice classification			
IEA Ice class	Meteorological icing	Instrumental icing	Icing loss
	% of year	% of year	% of gross annual production
5	>10	>20	>20
4	5-10	10-30	10-25
3	3-5	6-15	3-12
2	0,5-3	1-9	0,5-5
1	0-0,5	<1,5	0-0,5

1.2.2 Consequences of Ice

There are various icing related effects on wind turbines, but this chapter will only cover some of the most essential that have been described in the literature. To simplify, the affected attributes are divided in three main areas; shortened lifetime of the turbine, risk of danger and performance.

Shortened life time

A wind turbine can have its technical life time shortened if it is exposed to conditions it is not designed for. Increased fatigue load can occur when ice accretion differs in one of the blades causing imbalance in the rotor. The imbalance can come from both mass and aerodynamic imbalance. With an unbalanced rotor, vibration and resonance may arise which over time can result in shortened life time of components due to e.g. fatigue fracture (Bredesen et al., 2017; DNV GL AS, 2017; Ganander & Ronsten, 2003).

Risk of danger

With icing conditions, ice accumulates over the whole wind turbine, but the moving rotor blades can accumulate heavier ice loads then stationary parts (Morgan et al., 1997). This could pose a severe danger for people in relatively close vicinity, as pieces of ice are known for breaking off and thrown from turbine blades due to gravity and mechanical forces (Wahl & Giguere, 2006). Maintenance personnel are more exposed to this risk then the general public as they will venture more often to wind farms. The ice parts can be large and impose a danger to the structure itself (Bredesen et al., 2017; DNV GL AS, 2017; Homola, 2011; Morgan et al., 1997).

Instrumental icing could lead to dangerous situations as important sensors being influenced by ice. The worst-case scenario could be under extreme winds where the controller malfunctions due to icing and fails to stop the turbine resulting in catastrophic failure (Homola, 2011).

Reduced performance

Ice accretion on rotor blades causes degraded aerodynamic performance and consequently reduced production (Bredesen et al., 2017). The influence on airfoils will be further presented in chapter 2. With severe icing, wind turbines may come to a complete stop which can be a result of various complications. Firstly, vibration from rotor imbalance can trigger a safety alarm forcing the turbine to a halt. Secondly, if there is a deviation between rotor torque and expected torque (based on wind speed) that is outside a predefined level, another alarm will trigger a shutdown of the turbine. Lastly, if the icing is severe enough, the ice may have changed the airfoils to an extent that the wind forces does not manage to rotate the blades (Homola, 2011). These complete stops will reduce production hours which again may influence the investments.

1.2.3 Monitoring

One of the first steps in wind farm projects is to map the wind resource potential. Cold climate related problems such as icing will therefore be central to monitor as it affects the performance of wind turbines and induces potential downtime.

The important aspects to monitor when it comes to ice on wind turbines are: intensity (rate), duration, frequency, severity (load) and type of ice. Ice density may also be an aspect of interest. Density and severity of ice may be used to calculate rotor imbalance. The duration of an ice event, shape and intensity combined with wind resource is important for the energy calculation and the economic impact (Bredesen et al., 2017; Homola, 2011).

When it comes to ice detection on wind turbines, the best location to validate ice is on the tip of the blade. This is due to the physical process where ice accretion is dependent on relative velocity of supercooled water droplets which occurs at the tip. The blade tip will also reach higher than the nacelle and potential experience low clouds even if the nacelle does not. This increases the ice potential for the blade tip (Homola, 2011). Monitoring ice accretion on stationary objects at hub-height, which is the main method for pre-operational wind farms, may therefore underestimate icing.

During project planning of wind farms, there have not been any guidelines for ice monitoring until IEA's recommended practice was published in 2017. The guideline presents a minimum and recommended requirement when building a wind farm site in CC with ice risk.

The minimum required practice from (Bredesen et al., 2017) when mapping ice conditions at a site is to measure meteorological or instrumental icing at or above hub height. Frequency of meteorological icing (periods where ice accretion is feasible due to meteorological conditions) should (according to the recommendations of IEA) be evaluated through use of a camera system. Instrumental icing (period where ice is visible on objects) should be measured with use of two anemometers, one heated and one unheated. Also, evaluate if extrapolation is needed from measure height to rotor height. The ice frequency should be long-term correlated with preferably 10 years or more as there are large interannual variations concerning icing.

Bredesen et al. (2017) recommended practice (in addition to minimum practice) is to assess both meteorological and instrumental icing frequency using camera system or other validated system. Maximum ice load, type of ice and intensity should also be measured. Multiple parallel ice detection methods should also be used to increase the data foundation and quality.

To monitor these parameters, there are various methods and detectors. For operational wind farms one can utilize wind speed measurements from an ice-free anemometer combined with power curves and estimate the production. For pre-operational wind farms ISO 12494 have often been used as a simplification when calculating ice on wind turbines. A turbine is represented by a standard cylindrical ice collector (ISO cylindric 1 m length and 30 mm diameter) and is monitored for ice formation (ISO 12494, 2017).

A study on ice detection methods and measurement of atmospheric icing were done by Wadham-Gagnon et al. (2015) which compared nine different methods. Some of the methods where the use of camera, liquid water content, relative humidity and temperature, freely rotating

ISO cylinder. They concluded that estimating atmospheric icing events based on relative humidity (RH) and temperature is not recommended. The method resulted in four times the value compared to other methods. However, it can be used to exclude periods of accretion where RH is under 80% (Bredesen et al., 2017; Wadham-Gagnon et al., 2015)

1.2.4 Modelling

Research has been carried out on icing models for ice accretion (TURBICE) and energy estimation due to icing (ICELOSS).

TURBICE is a numerical model which is based on a theory from Makkonen (2000). It simulates ice accretion on wind turbine blades with respect to intensity and shape of the ice. Glaze and rime ice due to in-cloud icing is considered in model as well (Makkonen et al., 2001).

A model for estimating production losses due to icing in an operational wind farm is developed by Byrkjedal et al. (2015) called IceLoss. The model assume energy production continues when ice accrete on rotor blades, and a direct relation between ice load on a standard ISO cylinder and the production losses. The model uses operational data from three wind farms (data from 2009-2011) and Whether Research and Forecasting model (WRF) ice calculation to form a two-dimensional power curve. The power is then a function of ice load and wind speed (Byrkjedal et al., 2015; Hansson et al., 2016).

1.3 Thesis Outline

The main objective of this thesis is to estimate potential production losses due to ice accretion on wind turbine blades at the pre-operational wind farm Kvitfjell in Norway. Ice events are analysed based on time historical data from met mast and evaluated against meteorological data to determined atmospheric icing. Three scenarios are established, a reference scenario without ice degradation, a medium reduced production and a substantial reduced production scenario. Due to limitation of workload and time, homogeneous icing through the wind farm is assumed. Computational fluid dynamics is then utilized to estimate the expected energy production with respect to ice losses.

The outline of the thesis is as follows. Chapter 2 presents theoretical background explaining relevant theory within wind power and ice physics. Chapter 3 describe the method of data processing with identification of icing events and CFD simulation of the energy production. Chapter 4 will present the results from the simulation before it is discussed and concluded in chapter 5 and 6.

2. Theoretical Background

In order to understand the challenges faced when estimating production losses due to icing on wind turbine blades, a clear understanding of the theoretical background is required. This chapter will give an overview of the relevant physical theories associated with wind turbines, icing events and Computational fluid dynamics (CFD) modelling.

2.1 Wind Turbine Energy Production

A wind turbine produces electric energy by converting kinetic energy of the wind into mechanical energy that is utilized in a generator. The kinetic energy of the wind can be described by,

$$E = \frac{1}{2} mV^2, \tag{1}$$

where m is the mass in [kg] and V [m/s]. By considering the swept area of a turbine, the mass of passing air can be expressed by $m = \rho AV$, where ρ is the density of air [kg/m^3], A is swept area [m^2] and V is the wind speed [m/s]. The power of the wind P [W] can then be expressed by substituting for m in equation (1),

$$P_{Wind} = \frac{1}{2} \rho AV^3, \tag{2}$$

which is the available power for the wind turbine to utilize.

Wind turbines extract kinetic energy by lowering the speed of air passing through the swept area. In practice, the wind hits the turbine blades and force them to turn around. If the turbine extracts all the kinetic energy, wind speed on the downside of the rotor would be equal to zero. This would result in an unrealistic high pressure in front of the rotor due to the wind hitting a "wall" of air and the wind cannot pass the swept area. Therefore, it is not feasible to extract all the kinetic energy since the wind need some energy left to move on. The maximum value of kinetic energy that can be extracted is therefore 59,3 % which is stated by Betz law. The theoretical power from the wind turbine can then be described by,

$$P = C_p P_{Wind}, \tag{3}$$

where C_p is the power coefficient with max value of 0,59 and P_{Wind} from equation (2). For a given wind speed, C_p is a function of tip speed ratio λ, which is the ratio between blade tip speed and free stream wind speed. λ is then given by,

$$\lambda = \frac{\Omega R}{V}, \tag{4}$$

where V is the wind speed, Ω is the rotational speed of the rotor and R the radius (Manwell et al., 2009). The turbine will be most efficient at the optimum tip speed ratio as it utilizes most of the wind at that point. At higher or lower wind speeds, wind will either be pushed around the rotor or straight through without the blade capturing it.

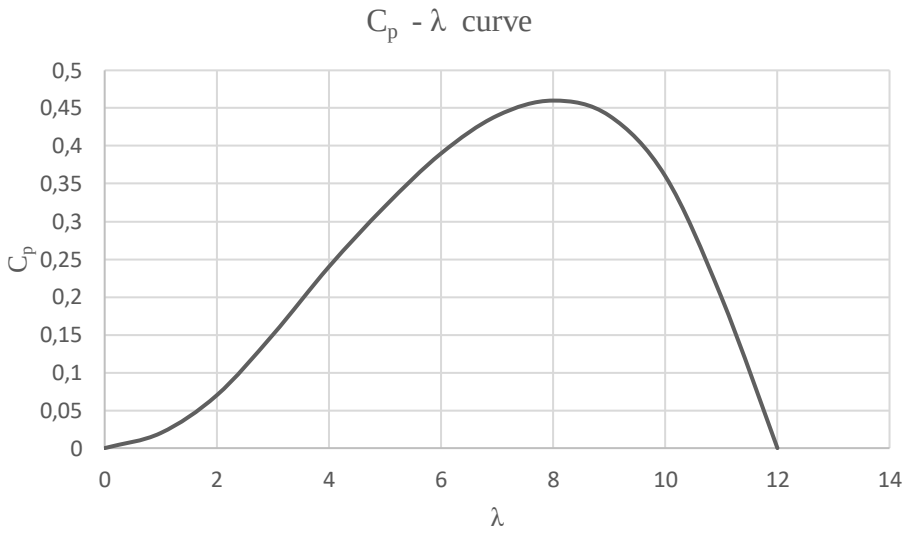

Figure 1: Example of an Cp-λ curve where power coefficient is a function of tip speed ratio.

From Figure 1 it can be seen that $\lambda = 0$ it will not be any energy production as the rotor will be still. At $\lambda = 12$ the rotor rotates so fast that the wind will see it as a solid disk and flow around. In between the we find the optimum value which will be where it extracts most energy from the wind. Because of this, turbines are developed with different C_P-λ curves depending on the wind conditions.

2.1.1 Aerodynamics

Turbine blades work with the same principal as found in airplane wings where there is drag and lift forces around airfoils. If one considers a fictitious plate, the drag force is the component that is lined with the air flow and will be largest when the air flow is perpendicular on the plate. The lift component is the force that is perpendicular to the air flow and is smallest when the

plate is lined with the air flow. If the plate has a small angle (angle of attack) relative to the wind direction, it induces a small pressure difference at the leeward side. This difference is a result of air traveling faster on the low-pressure/leeward side and it is a direct correlation between wind speed and pressure- higher wind speed leads to lower pressure. It is the lift force that is the main driver of a wind turbine (Boyle, 2012).

2.2 Icing Physics

To understand the impact of ice on turbine blades it is necessary to understand how ice develops and how it behaves, but before that it is necessary to define some terminologies.

An icing event has many stages which is equal regardless of icing type and can be defined in various ways depending on which point of view. From Figure 2 the different phases (incubation, accretion, persistence/ablation) in relation to meteorological-, rotor- and instrumental icing. For simplicity, this project is only going to refer to terminologies concerning instrumental icing.

Instrumental icing is defined by IEA as the period where ice is present/visible on structures and/or a meteorological instrument. An ice event may be described by three terms, accretion time, persistence time and ablation time. Accretion time is the time where ice is growing on a surface. Persistence time is the total duration ice remains on a surface without growing and ablation is the time where ice is removed natural through melting, sublimation, erosion and shedding (Bredesen et al., 2017). Illustration of the defined ice event is shown in Figure 2 in relation to meteorological icing and rotor icing.

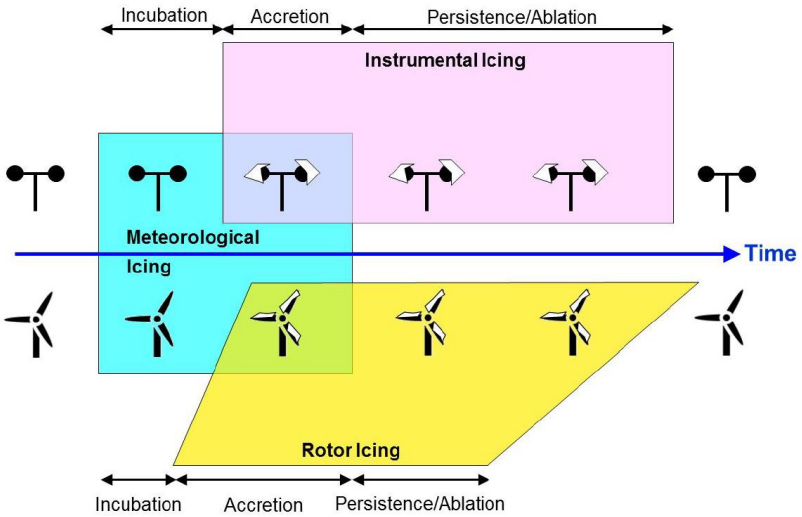

Figure 2: Definition of instrumental icing compared with rotor icing and meteorological icing (Bredesen et al., 2017).

2.2.1 Meteorology

The atmosphere is continuously in motion where there are several processes occurring such as evaporation, convection, condensation and precipitation. The main driver is solar radiation which heats up the surface causing convection with circulating air currents or parcels. Depending on temperature and relative humidity, the outcome of the convection can be clouds, ice crystals, condensation, supercooled droplets and many more to mention some.

When a moist air parcel is lifted, the pressure decreases, and the gas expands resulting in a lower temperature. At some point the parcel will become fully saturated of vapor and condensation enables water droplets formation. Droplets will usually form by condensation on small particles in the atmosphere called cloud condensation nuclei (CCN). The CCN will often not freeze until they are cooled down to -40°C. This is due to a relative immense surface energy at small cloud droplets which hinders ice formation since ice have a larger volume than water and the surface force does not allow the expansion. Therefore, the CCN will be emerged in water and form a supercooled droplet until reaching -40°C (depending on droplet size) or the surface is broken relieving the containing pressure causing an instantaneous freezing. Ice formation also occur above -40°C if there are ice nuclei present that can trigger the droplets to freeze by disrupting the surface energy.

2.2.2 Orographic Lifting

Orographic lifting occurs when air parcels are forced from low elevation to higher elevation due to topography such as e.g. mountains as illustrated in Figure 3. When the air parcel is lifted, it experiences a rapid cooling resulting in an increased liquid water content[1] (LWC). The LWC is therefore higher over hills and ridges than what would be expected from parcels at the same elevation above levelled terrain (Rogers & Yau, 1989).

[1] Liquid water content is the mass of water in an air parcel [g/m^3] as opposed to RH which is the ratio of water vapor to equilibrium vapor pressure.

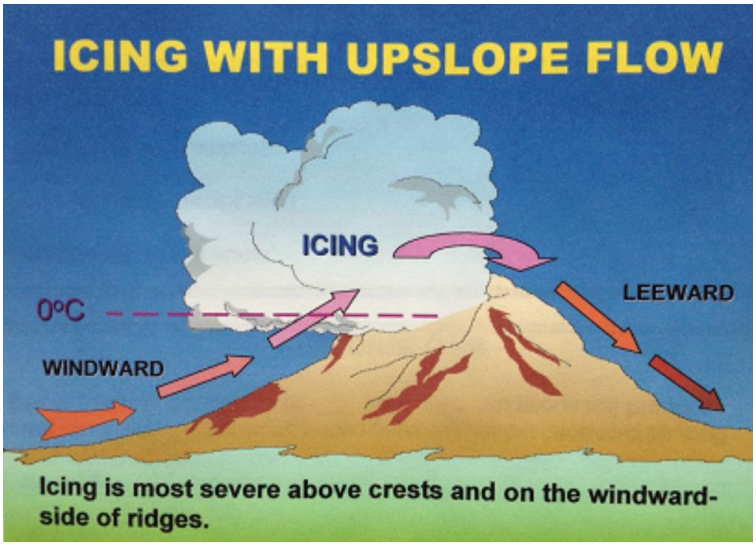

Figure 3: Illustration of orographic lifting (National Wheater Service).

A study from Makkonen and Ahti (1995) on effects of elevation on rime ice finds a strong correlation between elevation in relation to surrounding terrain than elevation to sea level. This could be an important factor to consider at Kvitfjell wind farm since wind turbines are placed on top of mountains on an island.

2.2.3 Ice Classifications

Ice can be categories based on different forms it takes and can be described as follows:

Glaze ice is a homogenous, transparent and smooth ice layer, shown in Figure 4, which often occurs between 0°C and -6°C and is caused by freezing rain, freezing drizzle or in-cloud icing. In short term, glaze ice is formed from water particles that does not freeze completely on impact with the surface. The non-frozen water can travel around the object and freeze on the leeward side (Bredesen et al., 2017).

Figure 4: Branches submerged in glaze ice (Perrault, 2009).

Rime ice occurs when supercooled liquid water particles hit the surface and freeze instantly. Based on the size of the particles and time of freezing, different types of rime ice can be formed. Small particles and fast freezing give a soft rime and larger particles with longer freezing time gives a hard rime. Since the supercooled water freezes instantly, there are no liquid water that can travel to the leeward side of the object, hence rime ice only occurs on the windward side of an object. Rime ice can occur down to -20°C but the ice growth often occurs at higher temperature and is asymmetrical (Bredesen et al., 2017). An illustration of rime ice on a wind turbine is shown in Figure 5.

Figure 5: Rime ice on a wind turbine (Ronsten, 2008).

Wet snow occurs with an air temperature between 0 and +3°C. At this condition, the snow crystals will partially be melted and therefore have a high water content. This will make the snow sticky and able to adhere to a surface (Bredesen et al., 2017).

2.2.4 Atmospheric Icing

Atmospheric icing is periods where atmospheric condition enables accretion of ice on structures exposed to the atmosphere. When considering ice accretion on wind turbines, there are two main type of atmospheric icing, precipitation icing (freezing rain or drizzle, wet snow) and in-cloud icing (glaze or rime ice) (Bredesen et al., 2017). However, the main cause of problem is ice from in-cloud icing with supercooled cloud droplets (Homola, 2011).

In-cloud icing

In-cloud icing happens when supercooled cloud droplets hits a surface and freezes. The droplets can freeze at different tempos depending on the thermal balance of the surface and therefore also give different characteristic to the ice. The thermal balance equation contains: energy released by the freezing droplets, evaporation, heat capacity of the forming ice/water layer, kinetic energy of incoming droplets, radiation, convection, conduction, and friction caused by the airflow.

When the heating flux is small, or the supercooling is large, droplets freezes immediate after meeting a surface and before next impinges. This results in an ice with lots of air gaps between the frozen particles and is called soft rime. If the freezing process goes slower due to higher heating flux or less cooling, less air will be trapped, and a stronger rime will be formed called hard rime. If the energy balance is such that the droplets does not freeze before the next impinges, a layer of water forms on the surface where the freezing occurs, and glace ice is formed. This ice has low amount of air and is therefore strong compared to the rime-ice (Homola, 2011; Rogers & Yau, 1989).

Precipitation icing

Precipitation icing can potentially lead to glaze ice or wet snow. The outcome depends on variation in temperature the precipitation experience. The variations can either be changes in temperature around ground level and a few hundred meters up, or rapid changes at one location.

Glaze ice can be formed through freezing rain or drizzle. This occurs when snow crystals are melted by warm air and form rain droplets, which then afterwards fall through a freezing layer of air close to the ground. It often happens in connection with temperature inversion where cold air is trapped underneath a layer of warm air. Wet snow can adhere onto a surface when the temperature is between 0°C and 3°C due to liquid water in the partial melted snow crystals. If the temperature subsequently decreases beneath freezing point, the accumulated snow will form ice (Bredesen et al., 2017; ISO 12494, 2017).

2.2.5 Droplet Trajectories

One important aspect of ice accretion is the number of droplets colliding with a surface. To describe the number of droplets hitting, or the collision efficiency[2], the size of droplets, velocity and size of object need to be considered (Lamraoui et al., 2014).

Droplets, or particles, will normally follow the airstream. However, when the wind hits an object the wind will bend around the object causing the particles to change trajectories. This can be illustrated by streamlines as shown in Figure 6 where the streamlines bend around the object. Small particles will follow the stream line quite easy, but larger droplets will not be influenced by the stream line at the same level due to larger mass and inertia, causing them to collide. Thus, air masses with large particles have a higher collision efficiency then air masses with smaller particles.

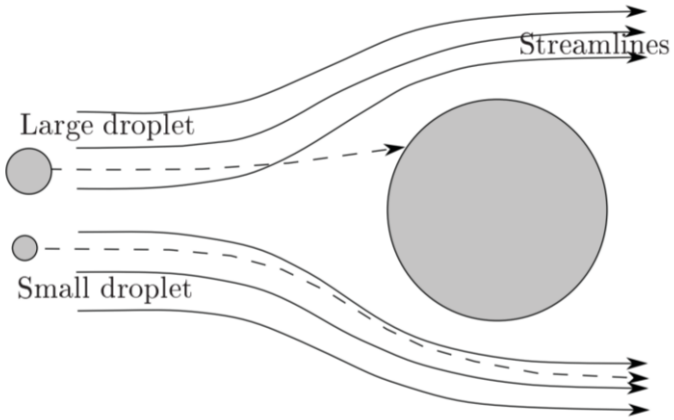

Figure 6: Droplet trajectories for small and big droplets (ISO 12494, 2017).

When air passes small objects, the streamline will not deviate as much as with larger objects. This makes it harder for particles to follow the streamline due to their mass and velocity, thereby more particles are hitting smaller objects. With larger objects, streamline will have a greater influence of the particles causing more to deflect (ISO 12494, 2017).

[2] Collision efficiency is a representation of the flux density of droplets hitting a surface in relation to total incoming droplets. It will always be less than 1,0 for airfoils due to the airstream bending around objects.

2.2.6 Ice on Rotor

Aerodynamic of rotor blades is essential for an efficient extraction of wind energy. The blades are designed for special working conditions with a clear airfoil. Changes in the airfoil can therefore lead to reduction in energy production. When ice accrete on a blade, the surface roughness increases causing a higher drag coefficient which again reduces the energy production (Lamraoui et al., 2014; Seifert & Richert, 1998). The changes in airfoil are generally represented by a reduction in lift coefficient (C_l) and increase in drag coefficient (C_d) and can be described by,

$$F_y = (C_l \cos\beta - C_d \sin\beta)\frac{1}{2}\rho v^2 c(r)\,, \tag{5}$$

where F_y is the rotating force, β is the inflow angel of the wind, ρ is the air density [kg/m^3], v is the wind speed [m/s] and c is the chord length [m] as a function of radius r (Homola, 2011). These changes can further be illustrated in Figure 7.

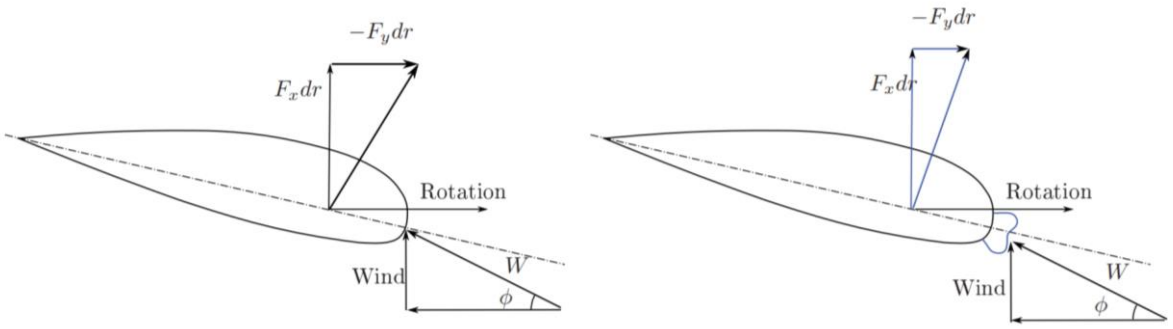

Figure 7: Illustration of airfoils with and without ice and the reduction in torque due to ice (Homola, 2011).

The influence from ice on turbine blades can vary, depending on the shape of the ice itself. Seifert and Richert (1998) have studied the performance of wind turbines with different ice-shaped airfoils and calculated the power curves, seen in Figure 8, on a fictitious wind turbine. According to them, the ice shape and quality may have a significant influence on the blade performance. The blade covered in 22% ice have a lower performance then a blade with 44% ice cover.

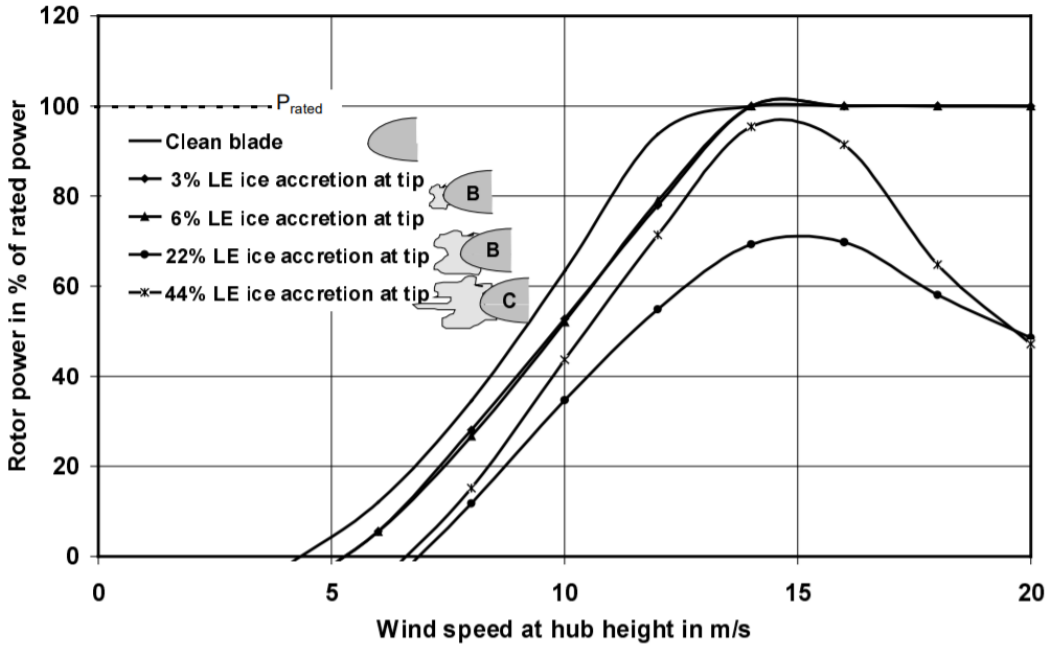

Figure 8: Calculated power curve for a pitch controlled fictitious turbine with different type of ice accretion (Seifert & Richert, 1998).

In this thesis, there is no knowledge about ice characteristics and the only validation of ice accretion is meteorological data from nearby weather stations and met mast.

2.2.7 Removal of Ice

During a melting process, ice will often melt unevenly resulting in ice falling off faster by shedding, especially at rotating blades (Morgan et al., 1997). Because of this shedding it is difficult to estimate when all ice is removed from the blades as the process is stochastic. Another important melting process is sublimation. This occur when the site is located in an area with long periods of temperatures below zero degrees. This process is not actually a melting process as the ice never melts, but changes state directly from ice to vapor. This can occur in a climate with dry and cold air which is typical climate for inland sites (Hansson et al., 2016).

2.3 Computational Fluid Dynamics

Computational fluid dynamics (CFD) is analysis and numerical problem solving of systems involving fluid flow (gas and liquids) by computer-based simulation. CFD has become a common tool within numerous fields such as hydrodynamics, hydrology and aerodynamics.

2.3.1 Assumptions

Computational fluid dynamics is based on three physical laws which is fundamental for all CFD models. They are stated by Versteeg and Malalasekera (2007) as follow:

- The mass of fluid is conserved
- Newton's second law: The rate of change of momentum equals the sum of forces on a fluid particle
- First law of thermodynamics: The rate of change of energy is equal to the sum of the rate of heat addition to and the rate of work done on a fluid particle

These laws are represented mathematically through governing equations.

2.3.2 Navier-Stokes Equations

The Navier-Stokes equations are fundamental in computational fluid dynamics as they calculate the behaviour of viscous fluid substance with respect to density, velocity, temperature and pressure (Versteeg & Malalasekera, 2007).

2.4 WindSim

WindSim is a CFD program used for simulating the behaviour of air flow as it passes over an area/landscape. It solves the atmospheric flow for a steady-state case at given initial and boundary conditions. To have a better understanding of the CFD simulation, the process can be divided into three steps; mathematical model, discrete model and discrete solution.

Mathematical model

The foundation of CFD in WindSim is a Reynolds-Averaged Navier-Stokes equation which is solved by combining numerous equations to describe the physical world. The Reynolds-averaged Navier-Stokes equations does not contain a turbulence component which therefore must be implemented by an external turbulence model. WindSim uses 2-equation turbulence models e.g. $k-\varepsilon$. In description of thermal stability WindSim uses a full coupling with a transport equation for temperature. The transport equation tells us how the temperature behaves in the domain. The momentum equation includes buoyancy (Gravdahl, 2019).

Discrete model

WindSim uses the finite-volume method were the flow domains are divided into smaller subdomains which forms a three-dimensional hexahedra grid. The refinement of the grid depends on how accurate the simulation is desired.

Discrete solution

Finally, each cell is solved through WindSim GCV solver (General Collocated Velocity) which acts as a guideline for equation order (Gravdahl, 2019). The model is solved by an iterative process and utilize the software packages PHOENICS.

3. Method

This chapter will first give a description of the site and data used for the energy production analysis before explaining the method used to simulate the total production and AEP influenced by icing.

3.1 Site Description

Kvitfjell wind farm is located in the northern part of Norway on the island Kvaløya south west of Tromsø city, seen in Figure 9. The project area spans over two mountains called Kvitfjell and Raudfjell which constitute the south west peninsula of the island. The site is located 300-550 meters above sea level with low vegetation. The climate is of a mild arctic characteristic with high precipitation. The winter last through five months, November to March, with an average temperature of -1,8°C (Yr.no, 2019). The site is exposed to harsh weather as it borders to the Norwegian Sea in west and the Barents Sea to the north which is known for polar low pressure weather systems. The total planned installed capacity is 281,4 GW divided on 67 turbines. The turbines are SIEMENS Gamesa's 4,2 MW WT-DD-130 R19. All turbines will have a hub-height of 85 m and a rotor diameter of 130 m.

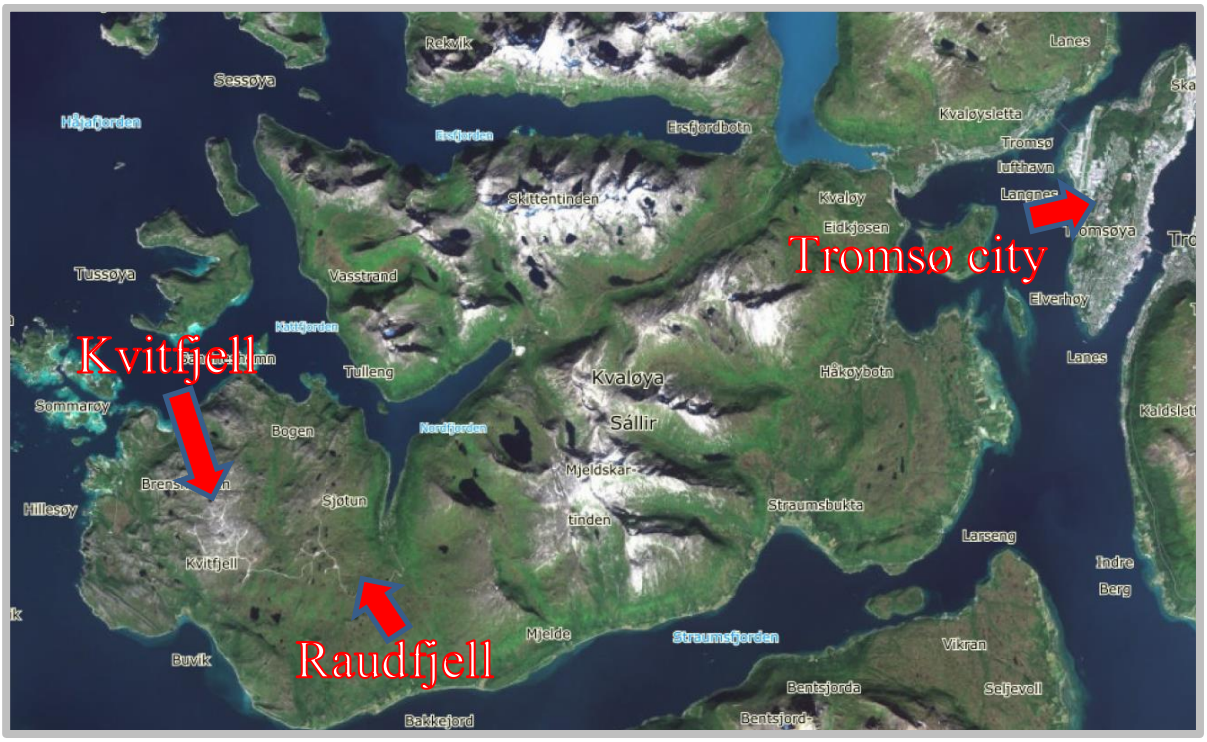

Figure 9: Kvitfjell wind farm in orientation to Tromsø city (Norge i Bilder, 2019).

3.2 Data Description

The estimation of ice losses are based on earlier measured data from two met masts, one at Kvitfjell at 551 meters and one at Raudfjell at 504 meters. The met masts are 80 meters tall with measure points at 40 m, 60 m and 80 m. Each elevation has heated anemometers (Vaisala) and unheated (Thies), wind vane (NRG Vane) is located at 40 m and 80 m, temperature and RH (Hygroclip) is measured at 4 m and 80 m, lastly the Ice monitor (SAAB) is located at 80 m. All data is recorded with 10 minutes interval between Julie 2014 and September 2016.

There are also data from Ultra Sonic 3D wind speed measure sensors, however they are not used in the analysis as they are not contributing with additional information on icing.

3.2.1 Data Filtering

The data is filtered by using Windographer and consist of four steps: 1. Initial filtering 2. Invalid filtering 3. Suspect filtering 4. Tower shadow filtering.

Initial filtering removes system errors during importing of met mast data into Windographer. Invalid filtering applies upper and lower limiting values and removes measured datapoints that does not satisfy the requirements. Range tests are applied to wind speed, direction, temperature and RH. Values outside the range of 0,1-80 m/s, 0-360 degrees, -50°C to 50°C and 0-100% RH is removed. Suspect filtering mark suspicious data to be examined further. Range test for mean wind speed above 40 m/s and constant test for mean direction less than 0,1 degree change over an hour is marked as suspicious. Tower shading filtering is applied for anemometers at the same height.

Due to malfunction of the 80 m (Thies) anemometer at Kvitfjell and temperature sensor at Raudfjell, the period from 1/1-2016 to September 2016. is removed from the dataset.

3.2.2 Identification of Ice Events in Met Mast Data

The most severe ice events are identified from met mast measure data by evaluating temperature, relative humidity, ice monitor and comparing heated and non-heated anemometer. If the criteria's seen in Table 2 are fulfilled, the event is categorized as an ice event.

Table 2: Ice event identification criteria

Sensor	**Criteria**
Temperature [°C]	T< 3
Relative humidity [%]	RH > 95
Ice monitor [g]	M > 200
Anemometer [m/s]	$V_{Thesis} < 0,2$ for more than three consecutive time steps and $V_{Vaisala} > V_{Thesis}$

Accretion time is added in advance and ablation time is added in the end of the persistence time. The accretion at the start of an ice event is based on an increasing deviation in speed between heated and unheated anemometers, accumulated mass on the ice monitor is less than 200 gram and RH are above 95 %. The phase last until the anemometer is frozen solid. The ablation at the end of an event is valid until the speed of unheated anemometer returns to the range of heated anemometers.

Due to inaccuracy in the ice monitor (there were long periods with negative values), the data is mainly used as an indicator of ice events. Other parameters are then used to evaluate the potential ice event. Events where heated anemometers also have been frozen is evaluated against meteorological data from eKlima to verify actual icing.

3.2.3 Dataset

Three datasets (.tws files) are exported for each met mast after filtering: normal, no ice and ice. The “Normal” contains measurements through the whole period. “No ice” have all ice events excluded and consist therefor of only “warm” periods. The last dataset, “Ice”, have excluded all the “warm” periods and contains only ice events. The different dataset is presented in Table 3. All three datasets are from heated anemometer and wind vane, both at 80 meters.

Table 3: Dataset overview

Dataset	Description
Normal	Complete time history with wind speed and direction from heated anemometers and wind vane.
No ice	Time history where ice events are excluded.
Ice	Time history of only ice events with heated sensors.

3.3 Energy Simulation

3.3.1 Scenarios Description

Three scenarios are defined for the estimation of production losses due to icing, one reference scenario and two ice affected scenarios. In the first scenario, the reference scenario, wind turbines do not experience any degradation from icing. The second scenario, named Reduced production 1, is a medium icing scenario with a reduced power curve and the third scenario is a heavily icing scenario, Reduced production 2. An overview of the scenario is shown in Table 4.

Table 4: Scenario description

Scenario	Description
Full production/Reference	No compensation for icing
Reduced production 1	Medium ice scenario. All turbines have their original power curve switched out with a reduced one. Assuming same ice intensity through the wind farm.
Reduced production 2	Worst case scenario. All turbines have their original power curve switched out with the worst-case scenario curve.

3.3.2 WindSim Modules

In the WindSim simulation it is only necessary to run the following modules: Terrain, Wind fields, Objects and Energy, as analysis of the sites suitability for wind farm is not within the scope of this project.

Terrain module

The digital terrain model is established with a maximum number of 500 000 cells and a refinement area with 20 cells in vertical direction. As shown in Figure 10, the refinement area has a higher resolution in the middle of the domain where the site is. Smoothening is not used and forest modelling is disregarded.

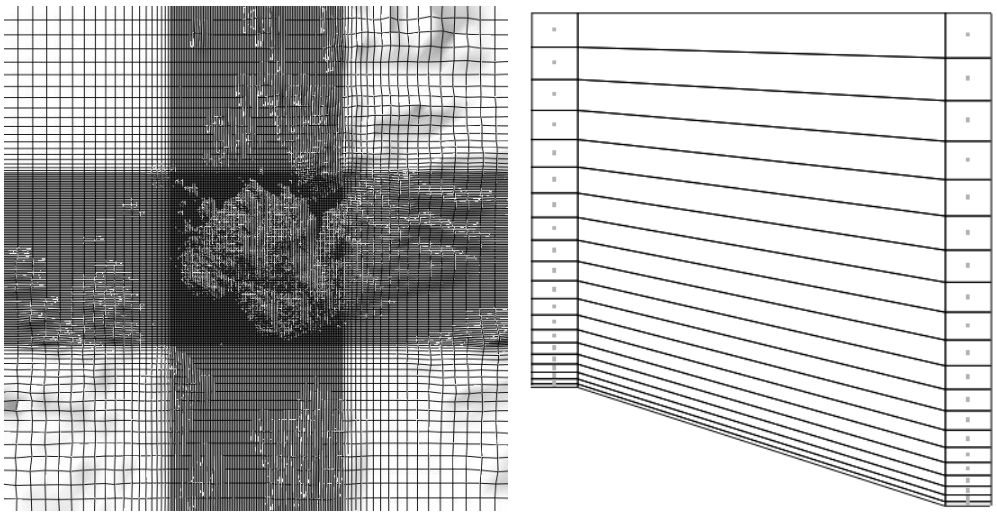

Figure 10: Grid with refinement area (to the left) and vertical (to the right) used in WindSim.

Resolution of the grid spacing at ground level in xy-direction is given in Table 5 where the total amount of cells in model is 499 280. The grid resolution in vertical (z) direction is given by the 10 closest cells relative to the ground, seen in Table 6.

Table 5: Grid spacing XY-direction

	x	**y**	**z**	**total**
Grid spacing, min - max [m]	113.0 - 1220.3	113.0 - 1220.3	Variable	-
Number of cells	158	158	20	499280

Table 6: Grid spacing Z-direction 10 closest cell relative to the ground.

.	**1**	**2**	**3**	**4**	**5**	**6**	**7**	**8**	**9**	**10**
z-dist. max [m]	14.7	51.2	101.7	166.1	244.5	336.8	443.1	563.4	697.7	845.9
z-dist. min [m]	19.4	67.5	133.9	218.8	322.1	443.8	583.8	742.3	919.2	1114.5

The topography of the domain is shown in Figure 11. In East and North-East region of the simulation area, a mountain dominated topography can be seen.

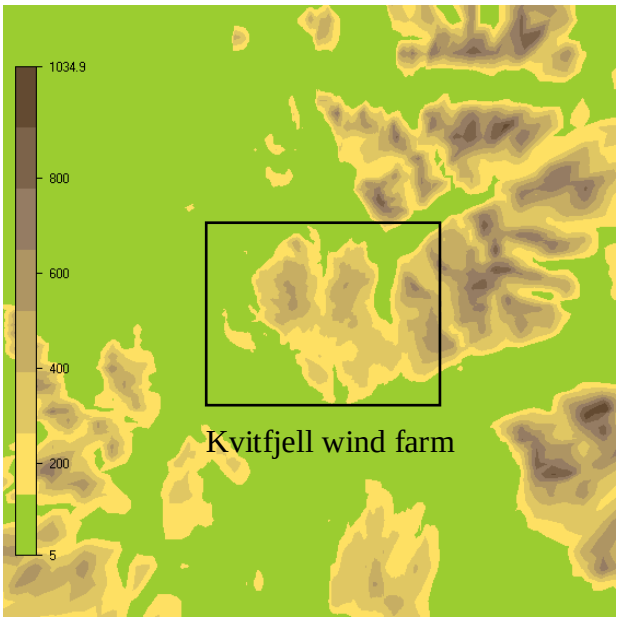

Figure 11: Digital terrain model with illustration of the wind farm– Elevation [m].

The roughness height is based on a gws-file received from the project owner. The roughness height through the domain is shown in Figure 12 where the value of 0,005 is dominating. Inclination angle is also seen in Figure 12 where there is a steep inclination around the site.

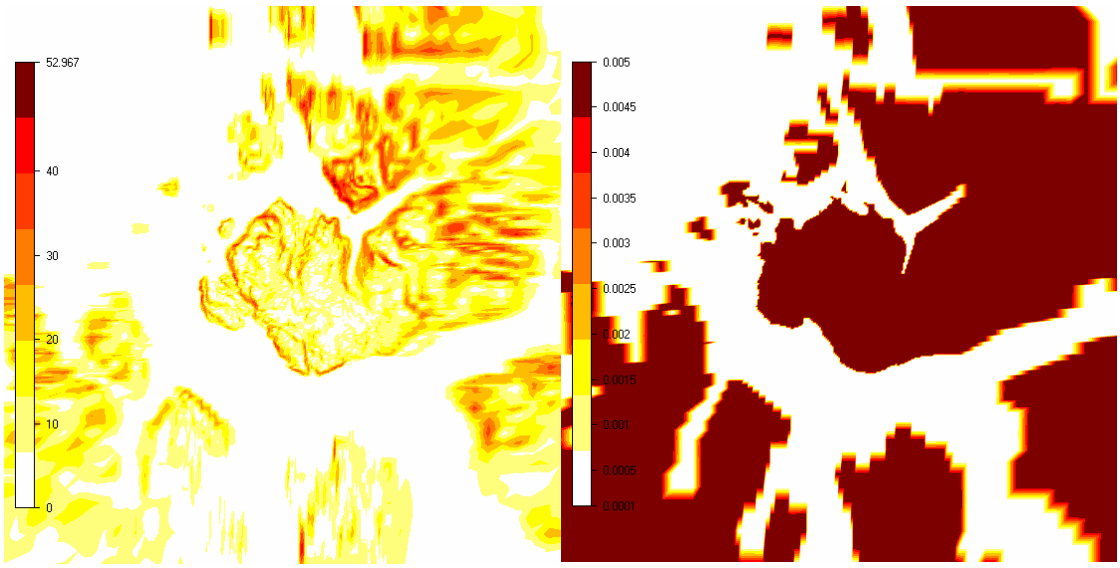

Figure 12: Digital terrain model - Roughness height [m] (to the right) - Inclination angle [deg] (to the left).

Wind fields

A wind field database is established by analysing 12 sectors with 30° degrees bins (+/- 15°). The sectors represent directions ranging from 0-359 degrees. For instance, sector 0 (355°-15°) correspond to wind from the north and 180 (165°-195°) correspond to south. The boundary layer height is set to 500 meters with a speed of 10 m/s above the layer. Fixed pressure is utilized as boundary condition at the top border. Temperature is disregarded, and air density is set to 1,225 [kg/m^3]. To model the turbulence, the RNG k-epsilon (ReNormalization Group) turbulence model is used with maximum of 500 iterations and convergence criteria at 0,005.

Objects

The total of 67 wind turbines is distributed between Kvitfjell and Raudfjell with 47 and 20 as shown in Figure 13. From the figure the placement of the two climatologies can be seen.

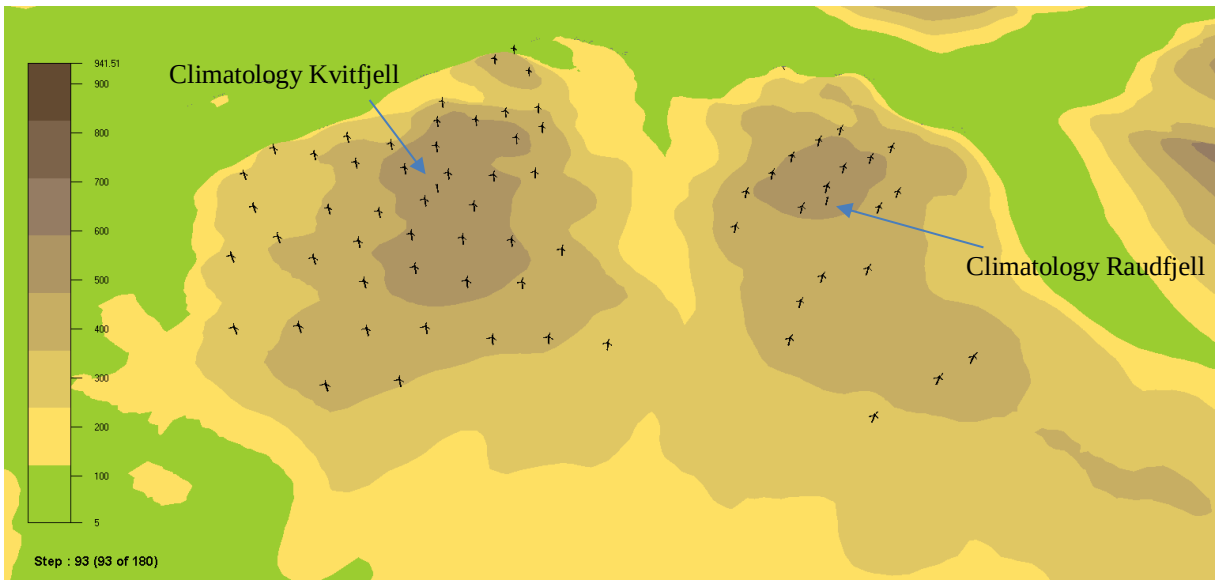

Figure 13: Wind turbine placements at Kvitfjell to the left and Raudfjell to the right.

It is assumed that all turbines located close to the met mast at Kvitfjell will experience the same ice intensity as the met mast. This will also be the assumption at Raudfjell. The two met mast may have experienced ice events at different periods. This may influence the weighting between the climatologies and give inaccurate data input to the turbines when considering the ice events. For example: turbines at Kvitfjell are experiencing ice events that belongs to Raudfjell. To avoid unwanted disturbance between the two climatologies, three layouts is established: L1, L2 and L3 as shown in Table 7. L1 consist of both Kvitfjell and Raudfjell together while Layout L2 and L3 consist only of turbines and climatology for Kvitfjell and Raudfjell respectively.

Table 7: Layout description

Layout #	Objects
L1	Kvitfjell and Raudfjell
L2	Kvitfjell
L3	Raudfjell

Total annual energy production for each scenario in the wind farm will consist of the combined energy estimate from Raudfjell and Kvitfjell (L1 or L2+L3) as illustrated in Table 8.

Table 8: Layouts divided by scenarios.

Scenario	Layout #	Description
Full production/Reference	L1	No compensation for ice
Reduced production 1	L2	Medium ice scenario. All turbines have their original power curve substituted with a reduced one. Assuming same ice intensity through the wind farm.
	L3	
Reduced production 2	L2	Worst case scenario. All turbines have their original power curve switched out with the worst-case scenario curve.
	L3	

To model the impact ice has on the ice scenarios, different power curves are used during the ice events. The reference scenario uses the original power curve from SIEMENS. Reduced production 1 uses a 50 % lower power curve then the original. The 50 % reduction is based on an illustrated power curve from SIEMENSs OWI data specification “Operation with Ice, SIEMENS G2 and D3”. Operation with ice (OWI) is an operation program during icing which is going to be implemented in the wind farm. Reduced production 2 will have a power curve equal zero to simulate full stop. The power curves are shown in Figure 14 whit the thrust coefficient.

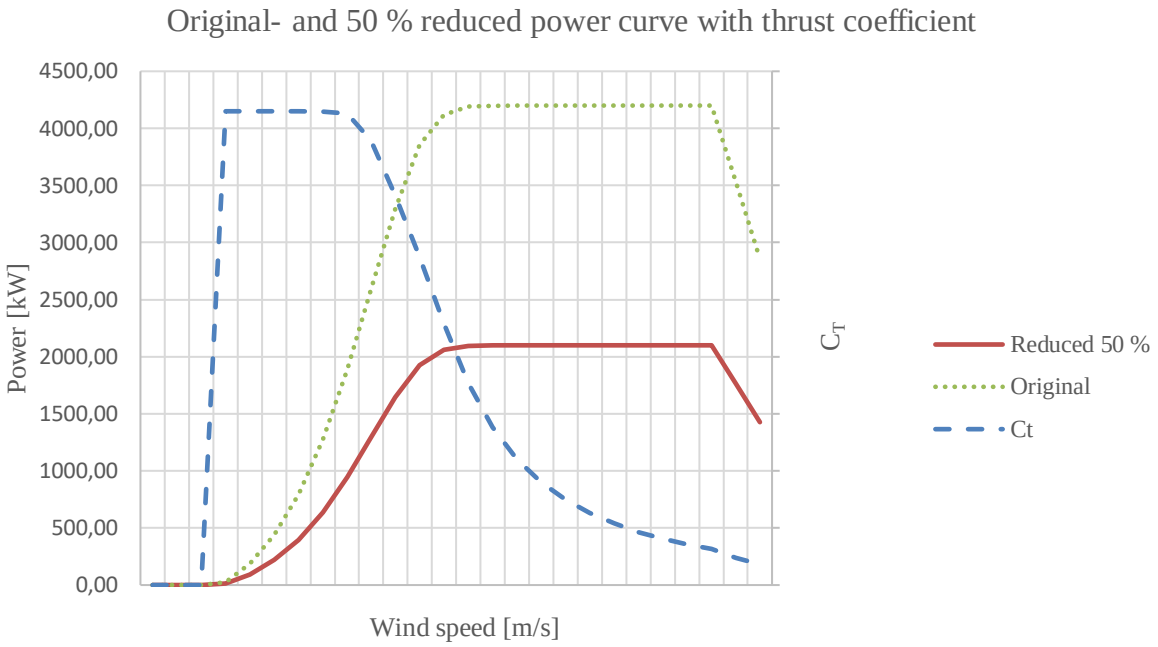

Figure 14: Power curves with thrust coefficient

Power curves with its corresponding scenario and layouts can be seen in Table 9. Both L2 and L3 needs to be simulated with the same power curve.

Table 9: Scenario with corresponding layouts and power curves.

Scenario	Layout #	Power curve	Description
Full production	L1	Original	No compensation for ice
Reduced production 1	L2	50 %	Medium ice scenario. All turbines have their original power curve substituted with the 50 % power curve in ice events. Assuming same ice intensity through the wind farm.
	L3	50 %	
Reduced production 2	L2	Complete stop	Worst case scenario. All turbines have their original power curve switched out with the worst-case scenario curve.
	L3	Complete stop	

A summary of the energy estimation process can be seen in Table 10. To have the total energy in each scenario, all the layouts must be estimated with its corresponding dataset and power curve. Power history is then exported from WindSim where the production in each time step is added up.

Table 10: Summary of energy simulation process.

Scenario	Layout #	Dataset	Power curve	Description
Full production	L1	Kvitfjell normal, Raudfjell normal	Original	No compensation for ice
Reduced production 1	L2	Kvitfjell no ice	Original	Medium ice scenario. All turbines have their original power curve substituted with the 50 % power curve in ice events. Assuming same ice intensity through the wind farm.
		Kvitfjell ice	50 %	
	L3	Raudfjell no ice	Original	
		Raudfjell ice	50 %	
Reduced production 2	L2	Kvitfjell no ice	Original	Worst case scenario. All turbines have their original power curve switched out with the worst-case scenario curve.
		Kvitfjell ice	Complete stop	
	L3	Raudfjell no ice	Original	
		Raudfjell ice	Complete stop	

Furthermore, the AEP in layout L1 is given by,

$$\mathrm{AEP} = \int_0^{\infty} \varepsilon(v)\varsigma(v)dv \quad , \qquad (6)$$

where $\varepsilon(V)$ is the power curve as a fuction of wind speed and $\varsigma(V)$ is the meassured frequenzedistribution of wind speed over a year (Barber et al., 2011).

Energy

During the calculation of energy production, the air density is corrected by “Individual 3” where density in each point is calculated. A temperature laps rate of -0,65 K/100 m and a pressure of 1013,25 hPa at sea level is applied with reference temperature 275,85 K at 0 meters (WindSim, 2019). Temperature gradient of -0,0065 K/m is used.

4. Results

4.1 Data Filtering

From the data filtering process there is identified 26 ice events at Kvitfjell and 12 at Raudfjell in the period of 17.07.2014 – 01.01.2016 which will be the foundation for the CFD-simulation.

The total hours of instrumental icing as a percentage of the year 2014-2015 (17.07.14-17.07.15) is calculated to 19 % and 6 % for Kvitfjell and Raudfjell respectively.

4.2 CFD-Simulation

Based on the filtered met mast measure data, the energy production is simulated for each scenario. The climatologies for Raudfjell and Kvitfjell are represented through wind roses as shown in Figure 15 where the frequency, direction and speed are given.

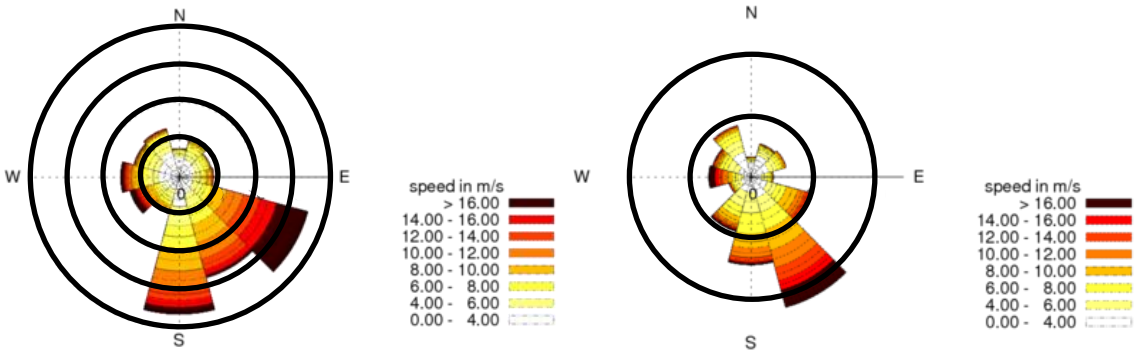

Figure 15: Wind roses for Kvitfjell (to the left) and Raudfjell (to the right).

The reference scenario with layout L1 results in an AEP which is 1,45 % higher than TÜVs own estimates when comparing gross AEP[3] from the frequency table without wake losses. The model is considered within reasonable range of accuracy. The different production on turbine level is shown in Figure 16 where K and R signifies turbines at Kvitfjell and Raudfjell. Turbine K28, which is the best performing turbine, have a 27 % better AEP than the lowest performing K50 (found between K5 and K6).

[3] The $AEP_{TÜV}$ is based on MCP climatology which is not done in this project. The AEP found in this simulation is only used to validate accuracy against TÜV.

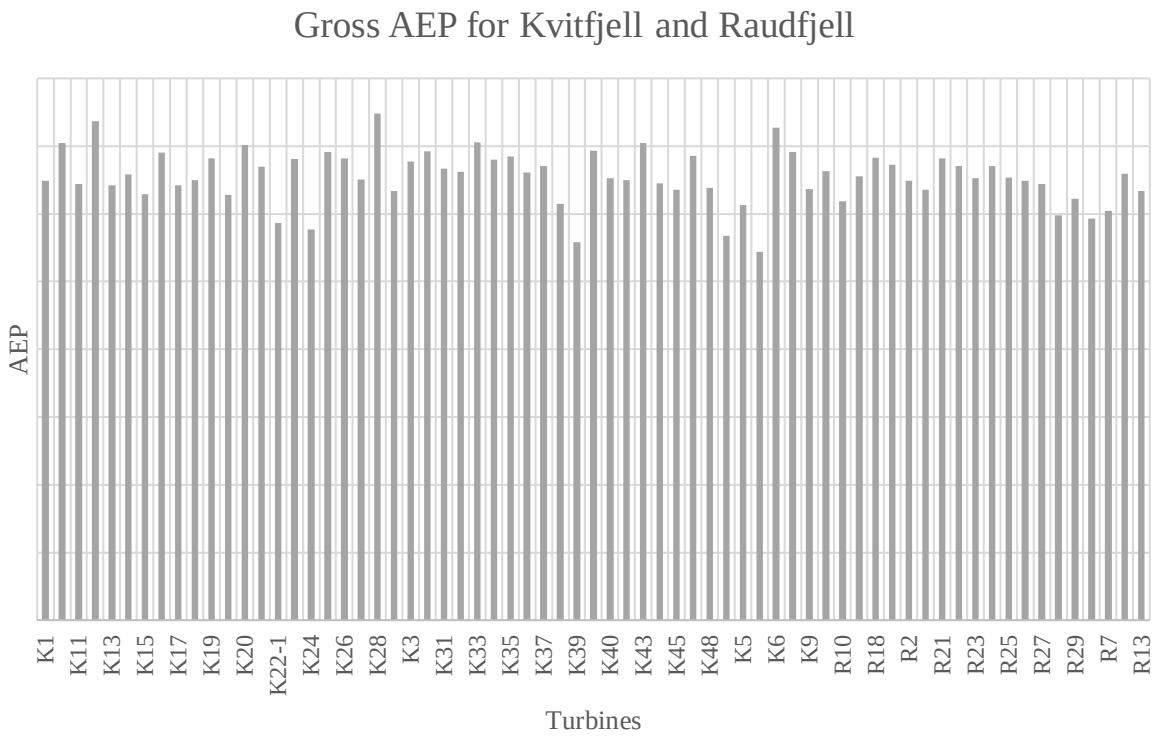

Figure 16: Variation in gross AEP for Kvitfjell and Raudfjell on turbine level.

In the scenarios Reduced production 1 and 2 the AEP is not considered as the dataset is not representative for a whole year when utilizing the frequency distribution. Therefore, the sum of all timesteps in the power history is used. The total energy from the power history is 6,89 % higher than the simulated AEP. It is the "Normal" energy production from power history which is used further in the comparison.

The "No ice" data set gives a production equal to 90,21 % of the "Normal" production at Kvitfjell and 91,19 % of normal production at Raudfjell. The energy production during ice events are estimated to be 4,89 % at Kvitfjell and 4,40 % at Raudfjell as shown to the right in Table 11 in scenario Reduced production 1.

Table 11: Total energy production in each dataset as a percentage of the normal production.

Scenario	Layout #	Dataset	Power curve	Total gross energy production %
Full production/Reference	L1	Kvitfjell normal	Original	100,00
		Raudfjell normal	Original	100,00
Reduced production 1	L2	Kvitfjell no ice	Original	90,21
		Kvitfjell ice	50 %	4,89
	L3	Raudfjell no ice	Original	91,19
		Raudfjell ice	50 %	4,40
Reduced production 2	L2	Kvitfjell no ice	Original	90,21
		Kvitfjell ice	Complete stop	0,00
	L3	Raudfjell no ice	Original	91,19
		Raudfjell ice	Complete stop	0,00

Kvitfjell has the highest production losses at 9,79 % compared to Raudfjell at 8,81 % in the worst-case scenario, as seen in Table 12 and Table 13.

Table 12: Production losses Kvitfjell as percentage of normal production.

	Total gross energy production %	
Kvitfjell	Reduced production 1	Reduced production 2
Production with ice	95,10	90,21
Losses due to ice	4,90	9,79

Table 13: Production losses Raudfjell as percentage of normal production.

	Total gross energy production %	
Raudfjell	Reduced production 1	Reduced production 2
Production with ice	95,59	91,19
Losses due to ice	4,41	8,81

The total production with ice on turbine blades is found by adding the production from the "no ice" and "Ice" dataset. During the period of 17.07.2014 – 01.01.2016 the total production losses due to icing is found to be 4,75 % and 9,50 % in Reduced production 1 and Reduced production 2 respectively as shown in Table 14. Down time due to maintenance is not considered.

Table 14: Total production losses due to icing

	Total gross energy production %	
Total	Reduced production 1	Reduced production 2
Normal production	100,00	100,00
Production with ice	95,25	90,50
Losses due to ice	**4,75**	**9,50**

5. Discussion

5.1 Data Filtering

After the filtering process the total of two winters where reduced to one and a half due to the removal of the data January-September 2016. This is unfortunate as there are large interannual variation in icing events (Bredesen et al., 2017) and it would have made a more accurate result to have two whole winters as a foundation of the analysis.

During the filtering there were some problems with the direction sensors where they were found to be locked in one direction over longer periods while others where shifting. These periods have been filtered out, but the lack of data in these periods may have influenced the frequency distribution for the AEP.

By comparing the percentage of annual instrumental icing at Kvitfjell and Raudfjell with the classification from IEA, production losses (based on gross annual production) of 10-25% and 3-12% may be expected at Kvitfjell and Raudfjell respectably. However, this is a rough approach which only gives an estimated and indication of what to expect. Further, the comparison may not be representative as it is only based on 1 year of data and should be compared against 10 years at least.

5.2 Identification of Ice Events

Identifying ice events and their duration as described in chapter 3 could possibly have over- and underestimated the icing effects. When considering the duration of the events, the main uncertainties comes from when the event starts and stops which is defined with the accretion and ablation time.

The start of the accretion time is defined by the ice monitor having accumulated more than 200 grams of mass and a distinct increase in deviation between heated and unheated anemometers. Due to the ice monitor being inconsistent in its measurements (often showing negative values) temperature and RH have also been used to define the start of accretion time. When using temperature and RH, the start is defined after reaching RH> 95 %, but it is unclear how long after the criteria is reached, the accretion time should start, resulting in uncertainty within the duration. The mismatch between ice formation on the monitor and actual icing on turbine blades may also deviate. The actual start of the accretion time could be earlier or later compared to what is defined in the method.

The end of the ablation time is based on unheated anemometer returning to the range of the heated. It is often seen that this is happening with ice shedding which contributes with uncertainties. The method used covers partly the process as the shedding presents itself quite clear in the data. However, there are uncertainties connected to shedding at different heights. From the data set it is observed variable shedding at the three different measure elevations both in advance and post shedding at 80 meters. If the sensors at 40- or 60 meters sheds before the sensor at 80 meters, it does not affect the duration of the ice event because the CFD-simulation is based on the time history at 80 meters. Due to this, the end of an ice event may occur later or earlier than what the shedding at 80 meters indicate thus affecting the duration of the ice event.

The same effect where data from 40- and 60 meters are neglected is applied to the speed measurements. If the anemometers at 40- and 80 meters is operating while 60 meters is frozen it is not considered an ice event. The icing conditions is then assumed to not be severe enough to influence the turbines performance.

Ice events where there are no solid frozen anemometers, but a deviation in range between heated and non-heated anemometer that suggest icing, is not considered a severe enough event to affect the production and therefor neglected. This can potentially underestimate the production losses if the aerodynamic properties are changed enough to influence the production in these periods.

5.3 CFD-Model

A CFD-model of the site has been established based on the earlier work from TÜV, but it is simplified to reduce the computational time. To keep the model as similar as possible the same gws-file is used in the new model. The roughness height is read from the gws-file which appears to be homogenous through the site. This may be too conservative with no variation in roughness, but the assumption is accepted as it is done by TÜV. It is also not known what the gws-file is based on and therefore difficult to establish any comprehensive analysis of the roughness height.

By establishing the separated layouts for Kvitfjell and Raudfjell, the simulation is carried out by preserving the integrity of the associated ice events and climatology. However, the general wind conditions could have been more accurate if there were used climatology at both places at the same time during the simulation and a weighting between each climatology.

If icing at turbine level had been considered, there are some turbine positions that should be examined further. One example is the turbines close to the edge of the plateau on the north side

of Kvitfjell. They could be more frequently exposed to icing conditions as they are located in an area with potential orographic lifting and higher LWC, contributing to higher ice losses.

5.4 Ice Modelling

The ice affected production is estimated through use of CFD and is modelled by changing the power curves of the wind turbines during icing events. The method has the advantage of showing how the potential production losses may be with given parameters in defined time periods. This could increase the accuracy of production estimates in shorter time periods compared to what could be expected from the long term statistical method as suggested by (Bredesen et al., 2017). By utilizing the method from this project, it is also possible to establish a more detailed sensitivity study on different icing potential by changing power curves.

On the other hand, there are a critical disadvantage as well. The correlation between ice on wind turbine blades and production losses is highly uncertain. This is due to lack of information of the actual ice formation at the site. Without this information it is not possible to connect ice shape and type to the ice modelling. The inclusion of these parameters could link the degraded aerodynamic properties to production losses, which could increase the accuracy of this method as described in chapter 2.2.6. This implies that it is not clear to what extent a power curve should be reduced to model the ice effect. It could be that a 70 % or 15 % reduced power curve is a more appropriate representation of the site than a 50 %, but by defining the different scenarios the extremal points is covered which may be of more importance for investors.

In reality, the wind turbines will have a gradually degrading power curve during the accretion time as the aerodynamic attributes are changing and a potential increasing power curve during ablation. In this project the new power curve, which is a flat reduction, is valid from the start of the accretion time inducing a potential overestimate of production loss. Due to the shedding effect the use of a flat reduction fits quite well at the end of an event.

The power curve should also be modelled different based on the ice event, as different ice events may have different ice formations and therefore different effect on the wind turbines. To account for this uncertainty, each ice event should be analysed, and an appropriate power curve should be designated.

In this project it is assumed homogeneous icing condition through the wind farm where the climatology data at met mast is extrapolated out to the turbine positions. By doing so, the variable atmospheric icing conditions is not considered where some turbines may not

experience any icing at all, but others have higher ice intensity. This add inaccuracy to the production losses. However, by modelling ice through the site on turbine level, this can be avoided.

The 4,2 MW installed turbines might also have reduced icing effects due to their size as described in chapter 2.2.5 where the trajectories of droplets are easier influenced by larger objects and deviates easier.

The effects from in-cloud icing is unknown as there have not been any camera system to log the cloud formations during the measure period. However, it can be expected that icing due to clouds will increase the losses further than what the results presented here indicates.

In ice events where the heated anemometer has frozen, it is assumed a severe ice event where the turbines must shut down. These events may still not be severe enough for the turbines to shut down, but there is no known wind speed at the site to simulate this condition.

An analyse of icing conditions at turbine level have been considered for this thesis, but due to being a to comprehensive task for a 30 ECT thesis, it was considered not feasible to conduct.

5.5 Energy Simulation

The three scenarios have been simulated in the CFD-program WindSim.

The deviation from TÜVs estimation in the reference scenario of 1,45 % is considered as an effect from the alternation of the CFD-model as it is reduced substantially. In the reduced production 1-scenario, the reduced power curve of 50 % is based on a drawing in a datasheet from the manufacture. This assumption of power curve may be conservative, but there are no other known approaches to define the “most likely” outcome scenario. In the reduced production 2 scenario it is assumed that the turbines are completely frozen and thereby not producing any electricity. This is done to create an extremal point and may not be considered the most likely scenario.

The deviation of 27 % in AEP between turbines shows that the CFD-simulation contribute to a more accurate AEP estimation of the wind farm as the variation is considered when utilizing CFD. Variation in the AEP is mainly due to different wind resources as wake losses is not considered. The variation in resources indicates that there are potential different ice conditions in the wind farm as ice intensity is also connected to velocity. This supports the choice of not assuming equal production at all turbines in the wind farm.

From the simulation of production losses, it is found that Kvitfjell has 0,98 % higher production loss than Raudfjell in the reduced production 2 scenario and 0,49 % higher in the reduced production 1 scenario. This difference may be due to higher amount of inclination areas close to the Kvitfjell met mast then what found around Raudfjell. The inclination may generally contribute to higher LWC at Kvitfjell due to orographic lifting and therefore more icing. Another reason may be the difference in elevation of the met masts. The met masts have a height difference of 47 meters which potential can alternate the atmospheric icing conditions.

Icing on wind turbine blades is known for its significant increase in aerodynamic drag and somewhat less aerodynamic lift. However, the reduced aerodynamic properties has, historically, often been exaggerated by the turbine control algorithm which regulates turbines as the rotor where ice free (Homola, 2011). As turbine controllers are improving (e.g. OWI), the production losses will mainly be due to aerodynamic performance degradation and not due to inadequate controllers (Homola, 2019).

6. Conclusion

Estimation of production losses due to icing has been carried out with data from met masts at Kvitfjell wind farm in the period of July 2014 to January 2016. A more concrete method of estimating ice losses has been established by utilizing CFD-simulation in comparison to the statistical approaches used by IEA.

The Computational fluid dynamic model's accuracy is compared to TÜVs own model and found to deviate 1,45 % which is considered within range of acceptance. Based on measurements from July 2014- January 2016, two scenarios are used to model different ice affected production. The most likely production losses to be expected is found to be 4,75 % of total energy production, but there are high uncertainties connected to annual variations in icing and therefore difficult to say anything about what to expect in the future. The maximum production losses are found in the worst-case scenario with a reduction of 9,50 %. When comparing the production losses at Kvitfjell and Raudfjell, Kvitfjell has 0,98 % higher losses than Raudfjell which is explained by different atmospheric icing conditions at the met masts.

There are considerable uncertainties within the ice modelling method as there are little knowledge of correlation between ice accretion and production losses. Due to this, simplifications and assumptions have been done such as homogenous icing through the wind farm and neglection of gradual reduced power curves. Further investigation on ice modelling should be done to increase the accuracy of production loss estimation.

7. Future Improvements

There are several improvements to the method that could increase the accuracy:

- Implantation of more data would reduce the uncertainty of interannual ice variations.
- Identification of variable atmospheric icing conditions on site to model icing at turbine level would increase the accuracy of estimates.
- Degrading power curve during accretion time needs to be investigated further.
- Shape and type of ice as well as cloud frequency could be investigated to increase the accuracy of the ice modelling.

If the proposed measures are instigated, the method may be utilized in the future to identify areas for improvement in the operation phase and the type of ice events that are most harmful to the turbines.

References

Barber, S., Wang, Y., Jafari, S., Chokani, N. & Abhari, R. S. (2011). The Impact of Ice Formation on Wind Turbine Performance and Aerodynamics. *Journal of Solar Energy Engineering*, 133 (1): 011007-011007-9. doi: 10.1115/1.4003187.

Boyle, G. (2012). *Renewable energy : power for a sustainable future*. 3rd ed. ed. Oxford: Oxford University Press/The Open University.

Bredesen, R. E., Cattin, R., Clausen, N.-E., Davis, N., Jordaens, P. J., Khadiri-Yazami, Z., Klintström, R., Krenn, A., Lehtomäki, V., Ronsten, G., et al. (2017). *IEA Wind TCP Recommended Practice 13 2nd Edition: Wind Energy in Cold Climates*: IEA.

Byrkjedal, Ø., Hansson, J. & Velde, H. v. d. (2015). *Development of operational forecasting for icing and wind power at cold climate sites*. Uppsala: Kjeller Vindteknikk AS.

DNV GL AS. (2017). *RECOMMENDED PRACTICE: Icing of wind turbines*.

Ganander, H. & Ronsten, G. (2003). *Design load aspects due to ice loading on wind turbine blades*. Boreas VI, proceedings of the international conference, Pyhätunturi, Finland.

Gravdahl, A. R. (2019). *WindSim CFD Procedure 1503*. WindSim training Basic Tonsberg: WindSim (12. February).

Hansson, J., Lindvall, J. & Byrkjedal, Ø. (2016). *Quantification of icing losses in wind farms: Assessment and optimization of the energy production of operational wind farms: Part 3*: Kjeller Vindteknikk.

Homola, M. (2019). (E-mail 30 January).

Homola, M. C. (2011). Atmospheric icing on wind turbines.

ISO 12494. (2017). *ISO 12494:2017*. Atmospheric icing of structures. Switzerland: International Organization for Standardization.

Lamraoui, F., Fortin, G., Benoit, R., Perron, J. & Masson, C. (2014). Atmospheric icing impact on wind turbine production. *Cold Regions Science and Technology*, 100: 36-49. doi: https://doi.org/10.1016/j.coldregions.2013.12.008.

Lehtomaki, V. (2016). *Emerging from the cold*. WindPower Monthly. Available at: https://www.windpowermonthly.com/article/1403504/emerging-cold (accessed: 14 October).

Makkonen, L. & Ahti, K. (1995). Climatic mapping of ice loads based on airport weather observations. *Atmospheric Research*, 36 (3): 185-193. doi: https://doi.org/10.1016/0169-8095(94)00034-B.

Makkonen, L. (2000). Models for the growth of rime, glaze, icicles and wet snow on structures. *Philosophical Transactions of the Royal Society of London. Series A: Mathematical, Physical and Engineering Sciences*, 358 (1776): 2913-2939.

Makkonen, L., Laakso, T., Marjaniemi, M. & Finstad, K. J. (2001). Modelling and Prevention of Ice Accretion on Wind Turbines. *Wind Engineering*, 25 (1): 3-21. doi: 10.1260/0309524011495791.

Manwell, J. F., McGowan, J. G. & Rogers, A. L. (2009). *Wind Energy Explained*. 2nd ed. ed. Chicester: John Wiley & Sons.

Morgan, C., Bossanyi, E. & Seifert, H. (1997). *Assessment of safety risks arising from wind turbine icing*. EWEC-CONFERENCE-: Citeseer.

National Wheater Service. *Icing*: National Wheater Service. Available at: https://www.weather.gov/source/zhu/ZHU_Training_Page/icing_stuff/icing/icing.htm (accessed: 25 Feburary).

Norge i Bilder. (2019). *Norge i Bilder*: Kartverket, NIBIO, Statens vegvesen. Available at: https://www.norgeibilder.no/ (accessed: 15 April).

Perrault, N. M. (2009). *Freezing Rain on Tree Branch*. Wikimedia Commons.

Rogers, R. R. & Yau, M. K. (1989). *A short course in cloud physics*. 3rd ed. ed. International series in natural philosophy, vol. 113. Oxford: Pergamon Press.

Ronsten, G. (2008). *Mapping of ice on wind turbine application- a feasibility study*. Elforsk rapport 08:40. Stockholm: Elforsk.

Seifert, H. & Richert, F. (1998). A recipe to estimate aerodynamics and loads on iced rotor blades. *proceedings of Boreas IV, Enontekiö, Hetta, Finland*.

Versteeg, H. K. & Malalasekera, W. (2007). *An introduction to computational fluid dynamics: the finite volume method*: Pearson education.

Wadham-Gagnon, M., Swytink-Binnema, N., Bolduc, D., Tété, K. & Arbez, C. (2015). *Ice Detection Methods and Measurement of Atmospheric Icing*. 16th International Workshop on Atmospheric Icing of Structures (IWAIS),, Uppsala. Québec, Canada: TechnoCentre éolien.

Wahl, D. & Giguere, P. (2006). Ice Shedding and Ice Throw–Risk and Mitigation. *General Electric Wind Application Engineering Group of GE Energy*.

WindSim. (2019). *Air density correction - Individual 3* (Version 9.0): WindSim.

Yr.no. (2019). *Climate statistics for Tromsø observation site.* In Jensen, I. S. (ed.). Yr.no: Norwegian Meteorological Institute

Norwegian Broadcasting Corporation. Available at: https://www.yr.no/place/Norway/Troms/Troms%C3%B8/Troms%C3%B8_observation_site/climate.month01.html (accessed: March 12.).

List of Figures

List of Tables

List of Equations

Kinetic energy of the wind	$E = \frac{1}{2}mV^2$	1
Power of the wind	$P_{Wind} = \frac{1}{2}\rho A V^3$	2
Theoretical power wind turbine	$P = C_p P_{Wind}$	3
Tip speed ratio	$\lambda = \frac{\Omega R}{V}$	4
Change in aerodynamic properties	$F_y = (C_l \cos\beta - C_d \sin\beta)\frac{1}{2}\rho v^2 c(r)$	5
Annual energy production AEP	$AEP = \int_0^\infty \varepsilon(v)\varsigma(v)dv$	6

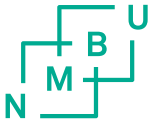

Norges miljø- og biovitenskapelige universitet
Noregs miljø- og biovitskapelege universitet
Norwegian University of Life Sciences

Postboks 5003
NO-1432 Ås
Norway